Materials Letters 308 (2022) 131144

Contents lists available at ScienceDirect

Materials Letters

journal homepage: www.elsevier.com/locate/matlet

A comparative study of front- and back-illuminated planar InGaAs/InP avalanche photodiodes

Yiren Chen [1], Zhiwei Zhang [1], Guoqing Miao, Hong Jiang, Hang Song *

State Key Laboratory of Luminescence and Applications, Changchun Institute of Optics, Fine Mechanics and Physics, Chinese Academy of Sciences, Changchun 130033, China

ARTICLE INFO

Keywords:
Epitaxial growth
Diffusion
Sensors
Semiconducting III-V materials
Avalanche photodiodes

ABSTRACT

In this work, a planar $In_{0.53}Ga_{0.47}As/InP$ avalanche photodiode (APD) working in both front- and back-illumination modes is fabricated for a comparative study. The great differences in the electrical and spectral performances between the two operating approaches can be originated from the PIN junction in the InP cap layer with high electric field, which plays the role of short-wavelength photoelectric conversion before the InP multiplication layer punches through under front-illumination.

1. Introduction

In comparison with a standard PIN or PN junction photodiode, the presence of internal gain in an avalanche photodiode (APD) can provide better sensitivity to satisfy the detection of extremely weak optical signals. [1,2] With the advent of autonomous driving technology, it puts forward an urgent requirement for eye-safe light detection and ranging (LiDAR). [3] Among the existing APDs, $In_{0.53}Ga_{0.47}As/InP$ APDs distinguish themselves with superior performances working in the short wavelength infrared region (0.9–1.7 μm), which covers the eye-safe wavelength for LiDAR. As one of the core devices in LiDAR system, the $In_{0.53}Ga_{0.47}As/InP$ APD with a separate absorption, grading, charge, and multiplication (SAGCM) heterostructure is the primary candidate (Fig. 1(b)). [4] In the described structure, an $In_{0.53}Ga_{0.47}As$ layer lattice-matched to the InP material is used to absorb photons at the wavelength of interest (e.g. the eye-safe wavelength of 1550 nm). It is adjacent to InP cap layer in which avalanche multiplication takes place. The charge layer is designed to regulate the electric field in the multiplication layer and in the absorption layer, enabling to provide sufficiently high electric field in the multiplication layer for desired avalanche probability and to keep low electric field in the absorption layer for minimal field-induced leakage current. [4,5] The photogenerated carriers in the absorption layer are separated and transported by the electric field, and the hole carriers in them may take place impact ionization effect in the multiplication region under high electric field (basically on the order of 10^5 V/cm) to form the carrier multiplication. Due to the existence of the depletion region in the InP multiplication region, it will act as a photon absorption layer before complete penetration under front-illumination. Thus, the $In_{0.53}Ga_{0.47}As/InP$ APD will present different photoelectric processes and characteristics under front- and back-illumination. Although independent studies have been conducted on both front- and back-illuminated $In_{0.53}Ga_{0.47}As/InP$ APD, no relevant works on their comparative study have been reported. Through comparative study, the performance difference of the same $In_{0.53}Ga_{0.47}As/InP$ APD under different working modes can be revealed, and the internal reasons involved can be also studied through the phenomenon. Moreover, an in-depth performance comparison between the two approaches has very important guiding significance for the application of the $In_{0.53}Ga_{0.47}As/InP$ APD.

In this letter, in order to demonstrate and evaluate the typical characteristics, a planar SAGCM structure $In_{0.53}Ga_{0.47}As/InP$ APD working in both front- and back-illumination modes is fabricated. The performance comparison is conducted and the photoelectric processes involved are also clarified in detail.

2. Experimental procedure

The SAGCM heterostructure material was epitaxially grown on a commercial 2 in. (1 0 0)-oriented sulfur-doped InP (n^+-InP) substrate by a metal–organic chemical deposition (MOCVD) system (Aixtron 200/4). During the growth, trimethylgallium (TMGa), trimethylindium (TMIn), arsine (AsH_3), and phosphine (PH_3) were used as the precursors for

* Corresponding author.
E-mail address: songh@ciomp.ac.cn (H. Song).
[1] These authors contributed equally.

https://doi.org/10.1016/j.matlet.2021.131144
Received 24 August 2021; Received in revised form 15 October 2021; Accepted 21 October 2021
Available online 26 October 2021
0167-577X/

epitaxy while silane (SiH_4) as the n-type dopant. For fabricating a planar $In_{0.53}Ga_{0.47}As$/InP APD, the p-type InP was first obtained by selective-area zinc diffusion method using a Zn_3P_2/Zn/SiO_2 multilayer as the dopant. After the SiO_2 cap was removed by inductively coupled plasma (ICP) etching method and the remaining Zn_3P_2 and Zn films were chemically removed by HNO_3 aqueous solution, a Ni/Ge/Au (50/20/200 nm) and a Ti/Pt/Au (50/20/200 nm) hollow square electrodes were evaporated on the n^+-InP and p-InP respectively by electron-beam evaporation to form n- and p-type electrical contacts.

The $In_{0.53}Ga_{0.47}As$/InP APD image was obtained by a metallographic microscope (Nikon, LV150). A high-resolution X-ray diffractometer (HRXRD, Bruker D8) was adopted to characterize the 2θ-ω scanning curve and the asymmetrical reciprocal space mapping (RSM) around (0 0 4) plane. The current–voltage (I-V) characteristics of the $In_{0.53}Ga_{0.47}As$/InP APD in dark and under illumination were measured by a semiconductor parameter analyzer (Agilent B1500A). The spectral response curves were obtained by a spectral response test system equipped with a standard InGaAs-based photodetector as the calibration.

3. Results and discussion

The $In_{0.53}Ga_{0.47}As$/InP APD material is grown by MOCVD at a reactor pressure of 10 kPa, and the structure is shown in the inset of Fig. 1(a). It is mainly consisted of a Si-doped n-InP buffer layer with a thickness ($t_{InP\ buffer}$) of 1 μm, an $In_{0.53}Ga_{0.47}As$ absorption layer comprised of an undoped $In_{0.53}Ga_{0.47}As$ layer ($t_{absorption} = 2$ μm) and a Si-doped n-$In_{0.53}Ga_{0.47}As$ layer ($t_{InGaAs} = 200$ nm), a lattice-matched InGaAsP grading layer with a total thickness ($t_{grading}$) of 120 nm, a 400 nm-thick Si-doped n-InP charge layer with a concentration of 5.0×10^{16} cm^{-3}, and an unintentionally doped InP cap layer with a thickness (t_{InP}) of 3.5 μm in sequence. The InGaAsP grading layer alleviates the energy discontinuity between n-$In_{0.53}Ga_{0.47}As$ layer and n-InP charge layer and avoids carrier accumulation in the heterojunction interface. Fig. 1 shows the (0 0 4)-plane 2θ-ω scanning curve of semi-log coordinates and its related reciprocal space mapping (RSM). The RSM (right inset) shows two main peaks corresponding to InP and $In_{0.53}Ga_{0.47}As$, and a gradient peak corresponding to the InGaAsP grading layer. The lattice mismatch ratio between the InP material and the $In_{0.53}Ga_{0.47}As$ material is estimated to be 0.0424%, indicating an almost lattice-matched epitaxy. Based on the epitaxial material, a selective-area zinc diffusion method is implemented to realize p-type doping in InP cap. [6,7] And the n- and p-type hollow square contact electrodes are fabricated by standard photolithography, electron-beam evaporation and lift-off processes. [8] The physical and schematic images of the double-sided incident (back- and front-illumination) planar $In_{0.53}Ga_{0.47}As$/InP APD are shown in Fig. 1(b) and inset, which has a photosensitive area of 40 μm × 40 μm on both sides.

In order to demonstrate the different performances of the planar $In_{0.53}Ga_{0.47}As$/InP APD under back- and front-illumination, the electrical properties are compared. Fig. 2(a) and (b) show its dark current and photocurrent as functions of bias voltage. The only difference is the former uses a full white light (tungsten halogen lamp) while the latter uses a 1550 nm-wavelength infrared light. The power density of both is about 500 $\mu W/cm^2$. It presents a low dark current below 0.55 pA at 90% of the breakdown voltage (V_b). The V_b is operationally defined as the voltage at a dark current of 10 μA [5,9] and it is about −40.4 V. In Fig. 2(a), the photocurrent of the device back-illuminated by a full white light starts to remarkably increase at the punch-through voltage (V_p) of about −20 V, where the depletion edge extends to the absorption layer. When the reverse voltage is higher than V_p ($V > V_p$), an extremely weak photocurrent is observed, indicating the photogenerated carriers in the absorption region cannot be effectively extracted to participate in impact ionization by its weak electric field under back-illumination. By comparison, the photocurrent of the device front-illuminated by a full white light is observed when $V > V_p$. However, in Fig. 2(b), the same trend of the photocurrent is observed no matter the device is back- or front-illuminated by a 1550 nm-wavelength infrared light.

The difference of the photocurrent between the two working modes can be intuitively understood from Fig. 3(a) and (c). We define the processes of photoelectric conversion in the $In_{0.53}Ga_{0.47}As$ absorption layer and the InP multiplication layer as PEC-I and PEC-II, respectively. Under back-illumination (Fig. 3(a)), due to the filtering effect of the n^+-InP substrate, mainly the photons with energy between the bandgap of InP ($E_g \sim 1.35$ eV) [10] and the bandgap of $In_{0.53}Ga_{0.47}As$ ($E_g \sim 0.75$ eV) [5] can occur photoresponse in the absorption layer (PEC-I process). Because of the weak electric field in it, the hole carriers can be effectively separated and transported to the multiplication region only when the reverse voltage is lower than V_p ($V < V_p$). Under front-illumination (Fig. 3(c)), there is a PIN junction in the InP cap layer that is sensitive to the photons with energy higher than the bandgap of InP. In other words, the wavelength of the photons shorter than $1240/E_{gInP}$ (about 920 nm) can be absorbed in the depletion region of the InP multiplication layer (PEC-II process). Due to the high electric field in the multiplication layer, the photogenerated carriers are easily extracted to form a photocurrent. The photons with energy lower than the bandgap of InP and higher than the bandgap of $In_{0.53}Ga_{0.47}As$ are possible to penetrate through the PIN junction of InP and be absorbed by the $In_{0.53}Ga_{0.47}As$

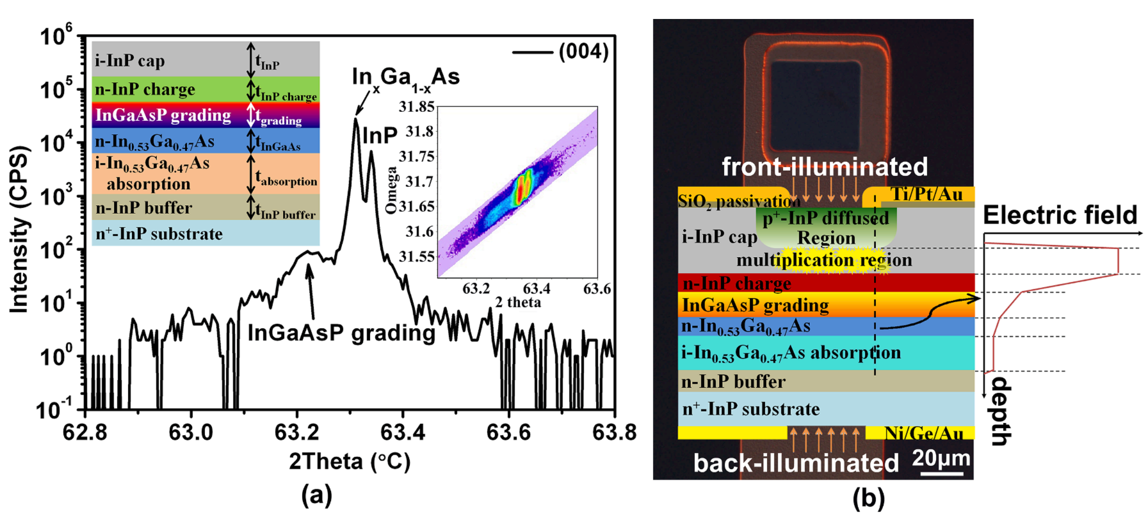

Fig. 1. (a) The (0 0 4)-plane 2θ-ω scanning curve and its related reciprocal space mapping (right inset). The left inset shows the material structure. (b) The physical image of the double-sided incident InGaAs/InP APD. Inset shows its schematic structure and the potential electric field distribution along the profile.

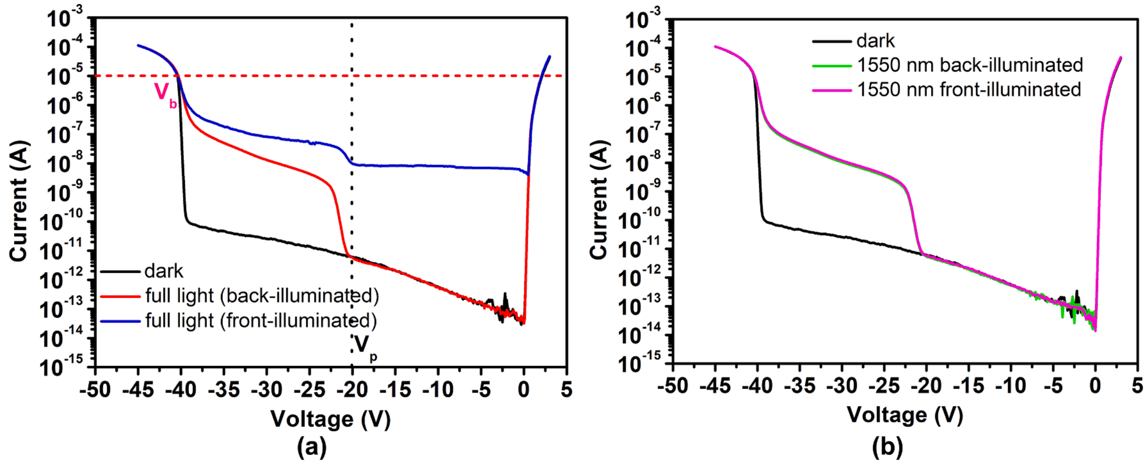

Fig. 2. (a) Comparison of electrical properties under dark, back-illuminated, and front-illuminated conditions using a full-spectrum light source. (b) Comparison of electrical properties under dark, back-illuminated, and front-illuminated conditions using a 1550-nm-wavelength light.

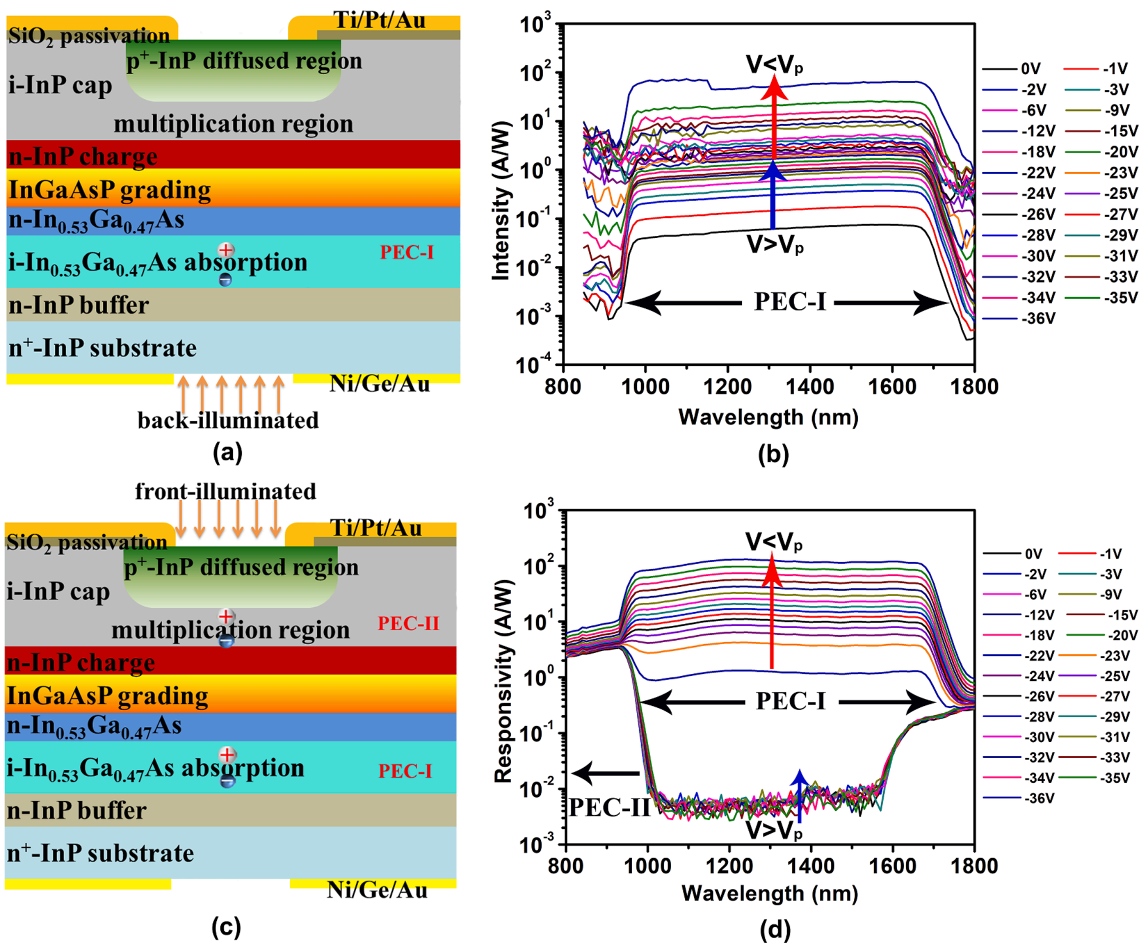

Fig. 3. The comparison of working process and spectral characteristic between the front illumination and the back illumination for the InGaAs/InP APD. (a) The spectral characteristics under front illumination and (b) its related illustration of working process. (c) The spectral characteristics under back illumination and (d) its related illustration of working process.

layer to supply the photocurrent (PEC-I process), especially after $V < V_p$. That is why the photocurrent presents throughout the whole reverse bias process and generates a step photocurrent at V_p, as shown in Fig. 2(a). The absence of the photocurrent from 0 V to V_p when the device is front-illuminated by the 1550 nm-wavelength infrared light (Fig. 2(b)) further confirms our analysis.

A comparative study of the spectral characteristics shown in Fig. 3(b) and (d) further exemplifies their photoelectric processes involved. It should be noted that the spectral response is measured up to 90% of V_b due to the current limitation of the phase-locked amplifier. As can be seen in Fig. 3(b), the spectral response curves of the $In_{0.53}Ga_{0.47}As$/InP APD in back-illumination mode only present a typical bandpass character, corresponding to the PEC-I process. Using V_p as the boundary line, the increasing rate of the spectral responsivity undergoes a process of low to high. By contrast, in Fig. 3 (d), when the reverse voltage is higher than V_p ($V > V_p$), the spectral response presents a short-wavelength response, mainly corresponding to the photoelectric conversion in InP (PEC-II).When $V < V_p$, it also presents a bandpass character the same as that of the device under back-illumination, corresponding to the PEC-I process.

4. Conclusions

In this letter, a double-sided incident planar SAGCM structure $In_{0.53}Ga_{0.47}As$/InP APD is fabricated for a comparative study. Through comparing the electrical properties of back- and front-illumination using a full white light and a 1550 nm-wavelength light, the difference in photocurrent confirms the important role of photoelectric conversion in the depletion region of the InP multiplication layer when the device is operated in the front-illumination mode. A comparison of spectral characteristics further exemplifies the short-wavelength response in the PIN junction of InP, in addition to the photoelectric conversion in the $In_{0.53}Ga_{0.47}As$ absorption layer.

CRediT authorship contribution statement

Yiren Chen: Conceptualization, Methodology, Data curation, Writing – original draft. **Zhiwei Zhang:** Data curation, Methodology, Investigation. **Guoqing Miao:** Validation, Resources, Visualization. **Hong Jiang:** Project administration, Resources. **Hang Song:** Supervision, Investigation, Writing – review & editing, Funding acquisition.

Declaration of Competing Interest

The authors declare that they have no known competing financial interests or personal relationships that could have appeared to influence the work reported in this paper.

Acknowledgment

This work was supported by National Key Research Program of China (Grant No. 2018YFF0109801).

References

[1] J. Zhang, M.A. Itzler, H. Zbinden, J.W. Pan, Light Sci. Appl. 4 (2015), e286.
[2] P. Bérard, M. Couture, R.J. Seymour, Proc. SPIE 11388 (2020) 113880P.
[3] Y. Li, J. Ibanez-Guzman, IEEE Signal Proc. Mag. 37 (2020) 50–61.
[4] R. Yang, Proc. SPIE 11763 (2021) 117631Z.
[5] M.A. Itzler, R. Ben-Michael, C.F. Hsu, K. Slomkowski, et al., J. Mod. Opt. 54 (2007) 283–304.
[6] F. Acerbi, A. Tosi, F. Zappa, Sensor. Actuat. A 201 (2013) 207–213.
[7] S. Wang, Q. Han, L. Hou, H. Ye, et al., Proc. SPIE 10843 (2019) 1084304.
[8] Y. Chen, X. Zhou, Z. Zhang, G. Miao, et al., Mater. Lett. 291 (2021), 129583.
[9] Y. Zhao, D. Zhang, L. Qin, Q. Tang, et al., Opt. Express 19 (2011) 8546–8556.
[10] V.K. Dixit, S. Kumar, S.D. Singh, S. Porwal, et al., Mater. Lett. 87 (2012) 69072.